CONF-881031--17

To be presented at the Eighth Topical Meeting on Technology of Fusion Energy, Salt Lake City, UT, October 9-13, 1988.

CONF-881031--17

DE89 000593

ACTIVATION CHARACTERISTICS OF DIFFERENT STEEL ALLOYS PROPOSED FOR NEAR-TERM FUSION REACTORS*

by

H. Attaya, Y. Gohar, D. Smith and C. C. Baker

Argonne National Laboratory
9700 S. Cass Ave.
Argonne, IL 60439

August 1988

*Work supported by the Department of Energy, Office of Fusion Energy, under Contract No. W-31-109-Eng-38.

ACTIVATION CHARACTERISTICS OF DIFFERENT STEEL ALLOYS PROPOSED FOR NEAR TERM FUSION REACTORS

H. Attaya, Y. Gohar, D. Smith, and C. Baker
Argonne National Laboratory
9700 S. Cass Avenue
Argonne, Illinois 60439 USA
(312) 972-4484

ABSTRACT

Analyses have been made for different structural alloys proposed for the International Thermonuclear Experimental Reactor (ITER). Candidate alloys include austenitic steels stabilized with nickel (NiSS) or manganese (MnSS). The radioactivity, the decay heat, and the waste disposal rating of each alloy have been calculated for the inboard shield of the ITER design option utilizing water cooled solid breeder blanket. The results show, for the 55 cm inboard shield and after 3 MW.yr/m2 fluence, that the long term activation problems, e.g. radioactive waste, of the MnSS are much less than that of the NiSS. All the MnSS alloys considered are qualified as Class C or better low level waste. Most of the NiSS alloys are not qualified for near surface burial. However, the short term decay heat generation rate for the MnSS is much higher than that of the NiSS.

INTRODUCTION

Several structural alloys are under consideration for fusion reactors to achieve the primary objective of low activation and safe fusion systems. An optimum choice for a structure material, subjected to the intense irradiation of the fusion environment, is the one that has high operational performance, long lifetime, minimum induced radioactivity, and is industrially and economically viable. The operational performance is measured in terms of the material strength; its resistance to radiation damage, corrosion, thermal fatigue, helium embrittlement etc.; and the ease of manufacture. Induced activation is usually quantified by the dose rate, the specific activity, and the afterheat. These and other associated quantities determine the impact of a fusion reactor on the environment and decide the requirements for the safe operation of the reactor and the safe disposal of the radioactive materials.

Activation level and type in a neutron irradiated material depend on the constituent elements of the material, the neutron spectrum, and the exposure time. As a results, it has been suggested that materials could be tailored to reduce the impurities and to substitute alloying elements identified as a major source of activation with other benign or low activation elements that have the similar alloying effects of the replaced one. For example, Ni could be replaced by Mn, Mo by W, and Nb by Ta.

In Austenitic steels, this substitution of element is rather complex, since the various alloying elements affect the stability of the austenite phase in different ways. For example, Mn is less effective than Ni stabilizing the austenite phase. Therefor, one must add more Mn than the replaced Ni. However, there is probably a limit on the allowable Mn concentration. It has been reported[1] that at concentration above 12%, the Mn stabilizing potency decreases and need to be augmented by stronger austenitising elements such as C or N. From the metallurgical standpoint, the latter is preferred because of its higher solubility in Mn and since the increase in C content leads to carbide precipitation which increases the risk of embrittlement and reduces corrosion resistance. However, N is the major source of the long lived ^{14}C isotope, and its concentration should be limited. Thus, optimizing the material composition to fulfill the above mentioned requirements, simultaneously, is quite complex.

* Work supported by the U.S. Department of Energy/Office of Fusion Energy

Furthermore, because the activation of material is due to the combination of the neutron cross-sections of the constituent elements of the material and the local neutron spectrum, the radioactivity of that particular material could vary from one fusion reactor design to another, and from one location to another location in the same design because of the change of the neutron spectrum. Thus, a material that has minimum activity in a design might not perform as well in another design. For this reason, one should be cautious in generalizing the activation results of a certain material in a particular design to other designs.

Based on the existing data bases, the austenitic stainless steel Type 316 has been selected as the primary candidate structural material for ITER. It is important, however, to consider the use of the low activation austenitic steels. This paper shows the impact of utilizing some of the proposed low activation steels in ITER in terms of the radioactivity, the waste disposal rating (WDR), and the decay heat.

ALLOYS' COMPOSITIONS

Two groups of stainless steel alloys are considered; the first is nickel stabilized steels (NiSS) including PCA, 316SS, and 304SS. The second group includes several proposed experimental and commercial manganese stabilized steels (MnSS). Table 1 shows the compositions of the alloys used in this work. The alloys Mn_a, Mn_b, Mn_c, Mn_d, Mn_e, Mn_f, and Mn_g are ORNL (Oak Ridge National Laboratory) experimental heats. The PCA has a more detailed chemical composition that includes many impurity elements. Available compositions for the other alloys are not as comprehensive as that of PCA.

As will be indicated later, Mn isotopes are responsible for major part of the decay heat of all these alloys. The Mn content (weight percentage) in NiSS ranges from 1.26% to 2%. In MnSS, the Mn content ranges from 10% to 21.13%. On the other hand, the concentration of Ni, which induces long term activation, ranges from 9.5% to 16% in NiSS, and only two MnSS (AMCR types) contain .26-.7% Ni. The percentage of C in the NiSS is from .005 to .058. All the MnSS alloys, except AMCR35, contain high carbon content which varies from .2 to .25%. The AMCR35 alloy contains .03% C. NiSS alloys contain .007 to .01% N, and only two of the MnSS alloys have about .055% N. Notice also the absence of Mo and Nb in the MnSS alloys.

GEOMETRY AND COMPOSITION

The water-cooled solid-breeder (WCSB) blanket concept, which is used in these calculations, is one of the US design options for ITER. In earlier phase of ITER design, the main machine parameters are 4.04 m major radius, 1.4 m minor radius, and 631 MW fusion power, and about 1.1 MW/m2 average neutron wall loading. The inboard shield thickness is .55 m. The WCSB inboard shield consists of three structural zones followed by one lead zone. The outer radius of the inboard first wall (FW) is 2.53 m. Moving inward; the first zone is 1 cm thick and has 70% SS (stainless steel), and 30% H2O; the second zone is 32 cm thick and has 90% SS, 10% H_2O; the third zone is 19 cm thick and contains 5% SS and 95% $TiHD_2$). The average neutron wall loading on the inboard is 1 MW/m^2. The WCSB outboard blanket consists of successive layers of steel, water, Be, and Li_2O followed by carbon reflector and steel shield.[2]

The neutron flux has been calculated using toroidal cylindrical geometry, in which the mutual neutronic coupling between the inboard and outboard blankets is included. Two transport calculations have been made, the first one uses the above stated inboard composition with Type 316SS. Fig. 1 shows the average neutron spectrum in the three inboard zones for this case. To show the effect of the neutron spectrum, the second transport calculation has been made such that the second inboard zone contains 80% W, 10% 316SS, and 10% H_2O. The neutron spectra in the inboard zones of this W-case are shown in Fig. 2.

The comparison of these two figures shows clearly the effect of W on the neutron spectrum and how effective the tungsten is in reducing the neutron flux in the third zone. Because the large inelastic cross section of W, however, the neutron population in the energy range of 1 keV to 1 MeV has increased in both the first and second zones. Consequently, neutron reactions favoring this energy range will increase.

The effect of using different steels on the neutron spectrum is neglected and the two neutron fluxes, calculated using 316SS, have been used for all other steels in the radioactivity calculations. Operation time of 3 full power years, yielding 3 MW-yr total

Table 1. Chemical Composition

	PCA	316SS	Mn_a	Mn_b	Mn_c	Mn_d	Mn_e	Mn_f	Mn_g	AMCR	AMCR35	T304p	T304r
B	0.005	0.	0.	0.	0.	0.	0.005	0.005	0.005	0.	0.	0.	0.
C	0.005	0.058	0.24	0.25	0.23	0.25	0.24	0.22	0.25	0.2	0.03	0.051	0.047
N	0.01	0.007	0.	0.	0.	0.	0.	0.	0.	0.06	0.05	0.031	0.031
Al	0.03	0.	0.	0.	0.	0.	0.	0.	0.	0.	0.	0.	0.
Si	0.5	0.46	0.	0.	0.	0.	0.	0.	0.	0.	0.	0.4	0.44
P	0.01	0.026	0.003	0.003	0.004	0.003	0.034	0.033	0.027	0.	0.	0.041	0.033
S	0.005	0.011	0.	0.	0.	0.	0.	0.	0.	0.	0.	0.016	0.015
K	0.0003	0.	0.	0.	0.	0.	0.	0.	0.	0.	0.	0.	0.
Ti	0.3	0.04	0.	0.11	0.	0.12	0.1	0.1	0.1	0.	0.	0.	0.
V	0.1	0.	0.01	0.01	0.01	0.01	0.01	0.1	0.1	0.	0.	0.	0.
Cr	14.	16.7	11.83	11.73	11.8	11.71	11.85	11.84	11.7	10.	14.1	18.5	18.6
Mn	2.	1.43	20.51	20.5	20.46	21.13	20.5	20.82	20.39	17.	19.9	1.37	1.26
Fe	64.8584	64.44	67.407	67.307	66.666	66.007	67.261	66.882	66.348	72.04	65.66	69.491	69.724
Co	0.03	0.03	0.	0.	0.	0.	0.	0.	0.	0.	0.	0.	0.
Ni	16.	13.9	0.	0.	0.	0.	0.	0.	0.	0.7	0.26	9.8	9.5
Cu	0.02	0.06	0.	0.	0.	0.	0.	0.	0.	0.	0.	0.	0.
As	0.02	0.	0.	0.	0.	0.	0.	0.	0.	0.	0.	0.	0.
Zr	0.005	0.	0.	0.	0.	0.	0.	0.	0.	0.	0.	0.	0.
Nb	0.03	0.	0.	0.	0.	0.	0.	0.	0.	0.	0.	0.	0.
Mo	2.	2.84	0.	0.	0.	0.	0.	0.	0.	0.	0.	0.3	0.35
Ag	0.0001	0.	0.	0.	0.	0.	0.	0.	0.	0.	0.	0.	0.
Cd	0.0002	0.	0.	0.	0.	0.	0.	0.	0.	0.	0.	0.	0.
Sn	0.005	0.	0.	0.	0.	0.	0.	0.	0.	0.	0.	0.	0.
Sb	0.001	0.	0.	0.	0.	0.	0.	0.	0.	0.	0.	0.	0.
Ba	0.001	0.	0.	0.	0.	0.	0.	0.	0.	0.	0.	0.	0.
Tb	0.001	0.	0.	0.	0.	0.	0.	0.	0.	0.	0.	0.	0.
Ta	0.01	0.	0.	0.	0.	0.	0.	0.	0.	0.	0.	0.	0.
W	0.05	0.	0.	0.09	0.83	0.77	0.	0.	1.08	0.	0.	0.	0.
Ir	0.001	0.	0.	0.	0.	0.	0.	0.	0.	0.	0.	0.	0.
Pb	0.001	0.	0.	0.	0.	0.	0.	0.	0.	0.	0.	0.	0.
Bi	0.001	0.	0.	0.	0.	0.	0.	0.	0.	0.	0.	0.	0.

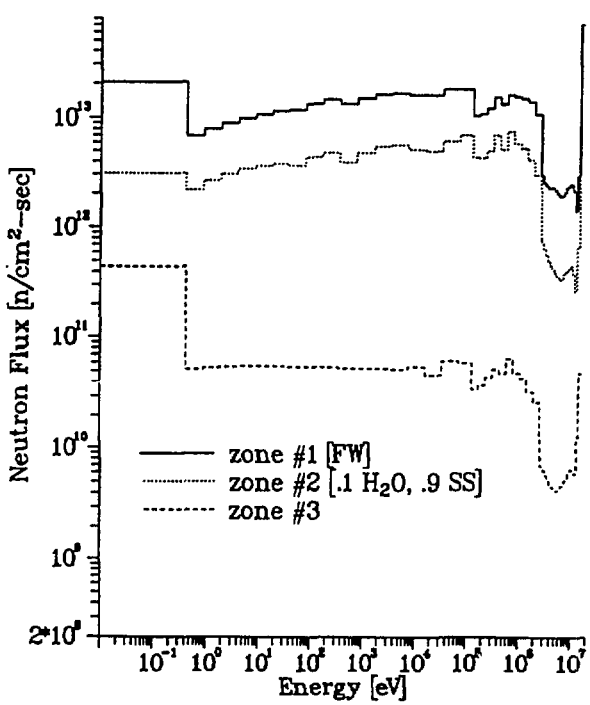

Figure 1
The neutron spectra in the all-steel case.

H. Page number

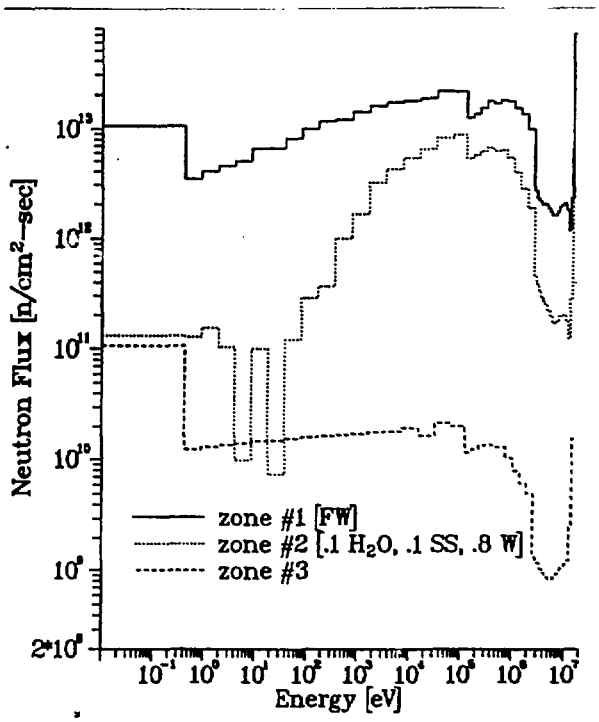

Figure 2
The neutron spectra in the W-steel case.

exposure, is used. The results shown here are for the structure only, and are given per cm of the blanket vertical length. The computer codes used in this work are the radioactivity code RACC[3] and the neutron transport code ONEDANT.[4]

RADIOACTIVITY

Consider first the MnSS alloys, the radioactivities of the alloys in this group, after reactor shutdown, are shown as a function of time in Fig. 3. The short-term activities are of the same magnitude, however, after 100 years, the activities of the AMCR alloy (.7% Ni, .05% N) and the AMCR35 alloy (.26% Ni, .06% N) are 4400 and 1500 times larger than the average activity of the ORNL alloys, respectively. The long-term activities of the AMCR alloys are largely due to the ^{63}Ni ($t_{\frac{1}{2}}$=100 yr), which is produced by the (n,γ) reaction with ^{62}Ni (abundance=3.5%) and the (n,2n) reaction of ^{64}Ni(abundance=.91%). The other part of the AMCR alloys long-term activities is due to ^{14}C which generated by the ^{14}N(n,p) reaction. These AMCR alloys' activities are, however, much less than that of the NiSS alloys as discussed later.

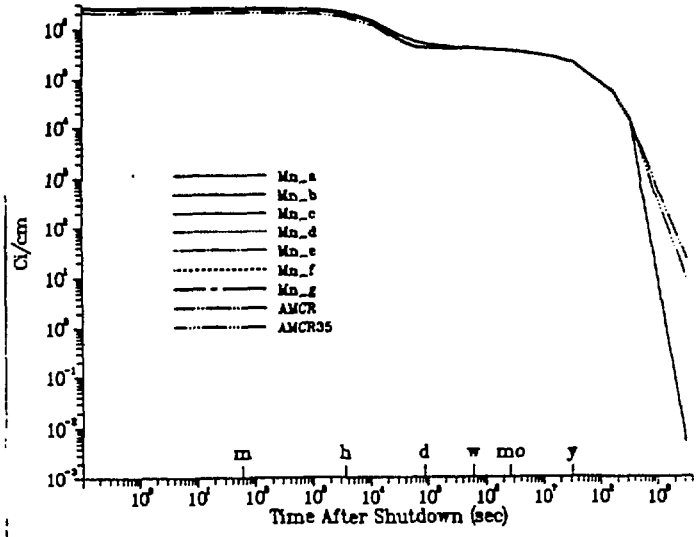

Figure 3
After shutdown radioactivities of the MnSS alloys.

For the ORNL alloys, the long-term activities, though very small, depend on the Fe contents, and are attributed to ^{53}Mn ($t_{\frac{1}{2}}$=3.7 x 10^6) yr), which is generated by the ^{54}Fe(n,d) reaction and the β^+ decay of ^{53}Fe($t_{\frac{1}{2}}$=8.5m) which in turn is produced by the ^{54}Fe(n,2n) reaction. In all the alloys, the ^{55}Fe isotope ($t_{\frac{1}{2}}$=2.7 yr; ^{54}Fe(n,γ), ^{56}Fe(n,2n), and ^{58}Ni(n,a)) dominates the activity in the period from 6 months to 10 years after shutdown.

To appreciate the differences in the short-term activities of the MnSS alloys, Fig. 4 shows the activities of these alloys relative to the activity of the Mn_a alloy which is also shown. At shutdown, the activities of the MnSS alloys depend on the Mn content and is dominated by ^{56}Mn($t_{\frac{1}{2}}$=2.6 hr) which is produced primarily (~ 88%) by the ^{55}Mn (n,γ) reaction and partly by ^{56}Fe(n,p), ^{57}Fe(n,d), ^{58}Fe (n,t), and ^{59}Co (n,a) reactions. Up to about 1 hour, Mn_d, which has the largest Mn content (21.13%), has the maximum activity. On the other hand, AMCR (the least Mn content of 10%), has the minimum activity for about 3 months after shutdown. After ^{56}Mn decays in about 10 hours, the ^{54}Mn isotope ($t_{\frac{1}{2}}$=312d; ^{55}Mn (n,2n) and ^{54}Fe (n,p) reactions) starts to dominate the activities of the MnSS alloys for about 5 years. Tungsten, if present, is responsible for the relative peaks at about 1 day. At that time and for the tungsten-MnSS alloys, the ^{187}W isotope ($t_{\frac{1}{2}}$ ~ 1 day; ^{186}W (n,γ) reaction) contributes about 25% to 30% of the activities of W-MnSS alloys; Mn_g, richest in W, has the maximum activity.

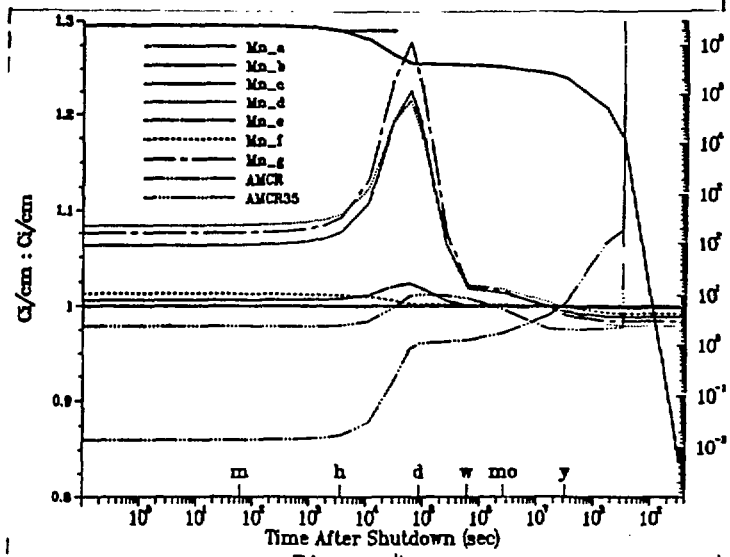

Figure 4
MnSS alloys' activities (left scale) relative to Mn_a's activity (right scale).

Consider now the NiSS alloys. The activity of the 316SS alloy is shown in Fig. 5 (right scale), and relative to it, the other alloys' activities are also plotted (left scale). Because the 304 steels have the least amount of Mn, Mo, Ni, and have no Nb content, they exhibit the minimum of both the short and long terms activities. PCA, richest in most

of these element (Mo, Ni, and Mn), yields the maximum activity most of the time and is exceeded only in the time interval from 1 year to 4 years by the 304 alloys which have the maximum Fe contents. The 304 alloys' activities transcends that of 316SS at about 1 month after shutdown and for about 10 years.

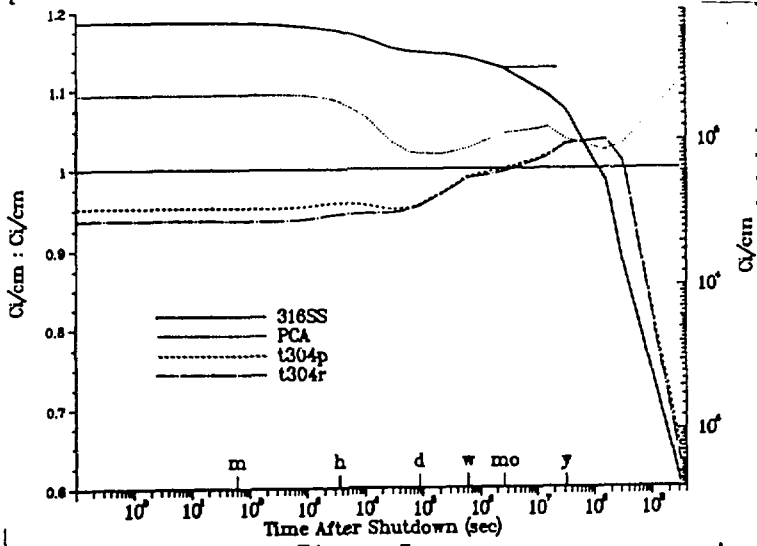

Figure 5

The NiSS alloys activities normalized to the 316SS activity (right scale-thick solid line).

At shutdown and for about 1 hour, the ^{56}Mn isotope generates more than 30% of the NiSS alloys' activities. The ^{55}Fe isotope produces ~ 50% (at ~ 1 day after shutdown) to 90% (at 5 years) of the NiSS alloys activities. At 100 years after shutdown, more than 90% of the NiSS alloys' activities is attributed to the ^{63}Ni isotope.

Other long-lived isotopes, that are important for the waste disposal rating and contribute to the activities of some of the NiSS alloys, are ^{94}Nb (mainly from Nb, and partly from Mo), ^{99}Tc (from Mo), ^{14}C (from N) and ^{59}Ni (from Ni). Thus, the presence of N, Nb, Mo, or Ni will render the materials radioactive for very long time and is detrimental in rating the waste of these materials as discussed shortly.

If the two groups are compared, Fig. 6, we find that the average activity of the MnSS alloys is factor of 3-4 larger than the average activity of the NiSS alloys for about 1 hour after shut down. After that, the relative difference decreases and at 1 day after shutdown the MnSS activities are about the same or slightly larger than the NiSS activities. After 1 day and for about 6 years, the MnSS activities remain higher than the NiSS activities, hereafter the MnSS activities start to decrease sharply and after 100 years, it become two (AMCR alloys) to five (ORNL alloys) orders of magnitude less than the NiSS activities.

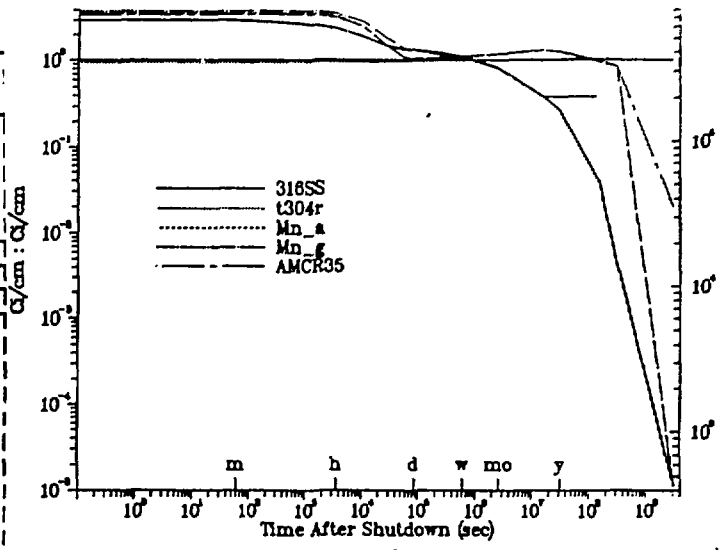

Figure 6

The activities of MnSS and NiSS alloys relative to the 316SS activity.

WASTE DISPOSAL RATING

The waste disposal rating of the alloys are shown in Table 2. These ratings are according 10CFR61.[5] The specific activity used to evaluate the WDR is equal to the total activity of the 3 zones divided by the sum of the volumes of the individual zones. To obtain the WDR of crushed (compacted) solid waste multiply the values in this table by 1.67.

Table 2. WDR

Alloy	Class	Value	Dominant Isotopes
Mn_a	A	2.49×10^{-5}	^{14}C(100.%)
Mn_b	A	2.59×10^{-5}	^{14}C(100.%)
Mn_c	A	2.38×10^{-5}	^{14}C(100.%)
Mn_d	A	2.59×10^{-5}	^{14}C(100.%)
Mn_e	A	2.49×10^{-5}	^{14}C(100.%)
Mn_f	A	2.28×10^{-5}	^{14}C(100.%)
Mn_g	A	2.59×10^{-5}	^{14}C(100.%)
AMCR	C	0.31	^{14}C(73.9%), ^{63}NI(25.5%), ^{59}NI
AMCR35	C	0.22	^{14}C(86.4%), ^{63}NI(25.5%), ^{59}NI
316SS	GTCC	2.3	^{63}NI(69.6%), ^{94}NB(25.1%) ^{14}C ^{99}TC(2.5%), ^{59}NI(1.6%),
PCA	GTCC	4.2	^{63}NI(69.6%), ^{63}NI(43.9%) ^{14}C(1.0%) ^{59}NI(1.0%), ^{99}TC
T304p	GTCC	1.3	^{63}NI(84.0%), ^{14}C(9.0%), ^{94}NB(4.5%), ^{59}NI(2.0%), ^{99}TC
T304r	GTCC	1.3	^{63}NI(82.9%), ^{14}C(9.1%), ^{94}NB(5.4%), ^{59}NI(2.0%), ^{99}TC

According to the 10CFR61 concentration limits, all the ORNL-MnSS alloys are classified as Class A waste. ^{14}C, generated by ^{13}C

(n,γ) reaction, is the only contributing isotope to the ratings of these alloy. Even if the wastes of these alloys are compacted, they remain Class A. The fact that the ORNL ratings are 4 orders of magnitude less than the maximum limit of Class A, would allow these alloys to meet the low level waste (LLW) Class C limits or better with reasonable amounts of impurities.

Because of the higher Ni and C contents in the MnSS-AMCR alloys, the radioactive wastes of these alloys, uncompacted or compacted, are classified as CLass C. The dominant isotopes in the ratings of the AMCR alloys are ^{14}C and ^{63}Ni. On the other hand, the WDR of all the NiSS alloys are greater than Class C (GTCC) and according to the present regulations, these alloys are unqualified for shallow land burial unless the irradiation time is reduced or waste dilution is allowed. Nickel, an essential alloying element in the NiSS steels, contributes 44% (in PCA) to 84% (in t304p) to the WDR of these steels. Substantial part of the WDR of the NiSS steels is due to N, Nb, and Mo. It is possible, however, for some of the NiSS alloys, e.g. 304SS, to meet Class C limit, if the inboard shield is mixed with the outboard blanket.

DECAY HEAT

Modified by the decay energies of the different isotopes, the profiles of the decay heat generation rate (DHGR) resemble that of the activities profiles. The DHGRs of different alloys, normalized to the DHGR of the 316SS, are shown in Fig. 7. Also shown in this figure are the DHGRs of W/316SS and W/Mn_a cases using the tungsten-316SS flux mentioned earlier. At shut down, the rate of heat generation in the MnSS alloys is 7 times that of 316SS and remains so for 1 hours. In this period, the manganese isotope ^{56}Mn produces 93% to 97% of the MnSS heat and about 73% to 78% of the NiSS heat. In the W/Mn_a case, the ^{56}Mn contribution drops to about 41% of the heat in the same period. From 1 day to about 3 years, the MnSS DHGRs are 1.5 to 2.5 times that of 316SS heat generation rate. The ^{54}Mn isotope is the dominant heat generator in the MnSS alloys, more than 97%, and is an important producer of the NiSS alloys' heat, about 20% to 40%.

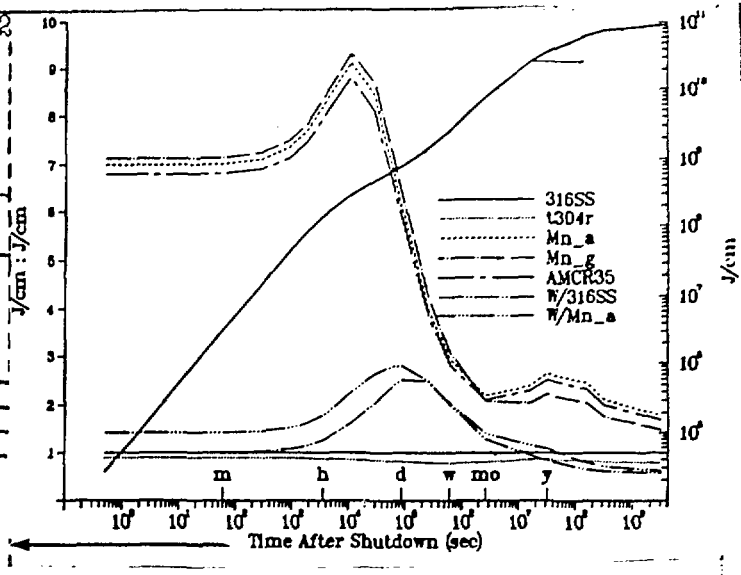

Figure 7
The DHGRs of different MnSS and NiSS alloys normalized to the 316SS DHGR.

How the material or the system responds to such rates of heat generation depends on the design details, and on the boundary and the initial conditions. In LOCA (Loss Of Coolant Accident) analysis, for example, adiabatic conditions are usually assumed to give a conservative estimate of the temperature of the materials. In this case, assuming that the MnSS and the NiSS alloys have similar thermal properties, the integration of the heat generation rates provides reasonable way to compare the temperature responses of the different alloys. Normalized to the integrated DHGR of the 316SS, the integrated DHGR of the alloys seen in Fig. 7, are shown in Fig. 8. As seen in Fig. 8, the accumulated heat in the MnSS alloys is 7 to 9 times that of the 316SS for about 3 hours after shutdown. After 1 month and for 100 years, the MnSS decay heat is more than twice that of the 316SS. This large difference in the accumulated energy, particularly in the first few hours, indicates that, in the case of LOCA, the temperature rise in the MnSS alloys would be much higher than in the NiSS alloys.

It is interesting to notice that in TIBER,[6] there was considerable concern about the decay heat generated in the W inboard shield. In Fig. 8, the integrated heat from the MnSS alloys is even higher than that of the W cases. However, the use of W with Mn_a has considerably diminished the accumulated decay energy in the inboard as seen in both Figs 7 and 8. This is attributed to the facts that there are less steel and less low energy neutrons in the W-case than in the all-steel

case. This suggests that if a high absorber such as W or B is used to compete for the thermal neutrons with the manganese, the afterheat of the MnSS alloys could probably be comparable to the 316SS afterheat.

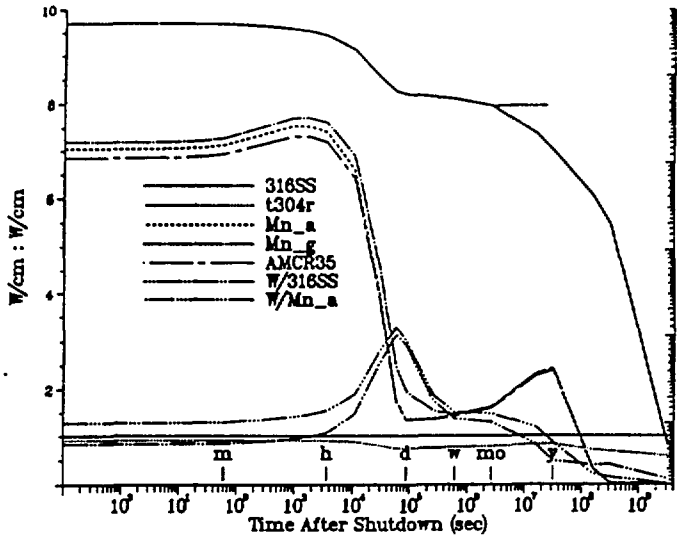

Figure 8
The integrated DHGRs of different MnSS and NiSS alloys normalized to the 316SS integrated DHGR.

CONCLUSIONS

Activation analyses have been made for two kinds of austenitic steels, nickel stabilized and manganese stabilized steels, after being used in the inboard shield of ITER. The radioactivity, the WDR, and the afterheat characteristics of the alloys in both groups have been discussed and compared.

The results show that the use of the MnSS alloys, in the inboard shield of ITER, provides considerable advantages with respect to the long-term activation problems. Unlike the NiSS alloys, the radioactive wastes of all the MnSS alloys considered are qualified for shallow land burial. However, the large amount of decay heat produced by the Mn isotopes, in the first few hours after shutdown, could result in large temperature rise in the structure in the case of LOCA unless an active and reliable safety scheme is employed. The decay heat in the MnSS alloys could be reduced, however, if high neutron absorbers are used to diminish the number of low energy neutrons.

REFERENCES

1. A.H. BOTT, F.D. PICKERING, and G.J. BUTTERWORTH, J. Nucl. Mater., 141-143 (1986), 1088.
2. U. S. NUCLEAR GROUP, ANL/FPP/88-1, Argonne National Laboratory Report (1988).
3. J. JUNG, ANL/FPP/TM-122, Argonne National Laboratory Report (1979).
4. R. O'DELL, et al., LA-9184-M, Los Alamos National Laboratory Report (1982).
5. Code of Federal Regulation, Title 10, Part 61, Washington, DC, Nuclear Regulatory Commission, 1982.
6. H. ATTAYA, 12th Symposium on Fusion Engineering, Monterey, California (1987).

AUTHOR INSTRUCTIONS

A. Title (all capitals, centered)
B. Title (if needed)
C. Author's name and company/organization
D. Street address or box number
E. City, state, zip
F. Telephone number
G. First line of paper
H. Page number

COLUMN 2